

ANALYSIS OF ISP-42, PANDA TEST WITH THE SPECTRA CODE

MAREK M. STEMPNIEWICZ

NRG, Nuclear Research and Consultancy Group
Utrechtseweg 310, 6800 ET Arnhem, The Netherlands
E-mail: stempniewicz@nrg-nl.com

Key words: Codes - Containment - Passive - Thermal-hydraulic - Two-phase

ABSTRACT

International Standard Problems (ISP) are organized in order to assess the ability of computer codes to predict the outcome of accidents in Nuclear Power Plants. The ISP-42 test was performed at Paul Scherrer Institute in 1998, as a sequence of six phases, Phase A through F. Blind and open calculations of ISP-42 were performed with the computer code SPECTRA for each of the six phases. SPECTRA is a general tool for thermal-hydraulic analyses.

Results of blind calculations are in good agreement with experiment. For open calculations several modifications were made in the model. These were mainly corrections of some input errors made in the model used for blind analysis. Some small improvements to the nodalization were made. Results of open calculations are generally closer to the experiment than the blind results. For phase D the containment pressure prediction was somewhat worse in the open calculation.

Based on comparisons of blind and open results with experiment several conclusions may be drawn:

- *use of long 1D structures, in contact with pool and atmosphere should be avoided,*
- *PCC units are better represented with larger amount of Control Volumes,*
- *two parallel junctions should be used to represent large openings between vessels, like drywell air line, etc.,*
- *careful verification of input decks is needed,*
- *stratification models in SPECTRA are useful for cases with light gas injection; for complex cases a complementary SPECTRA-CFD analysis may be performed.*

1 INTRODUCTION

International Standard Problems (ISP) are organized in order to assess the ability of computer codes as well as their users to predict the outcome of accidents in Nuclear Power Plants. The ISP-42 test was performed at Paul Scherrer Institute (PSI) on April 21/22, 1998. This ISP was run under auspices of the OECD NEA Committee for the Safety of Nuclear Installations (CSNI) and was financially supported by the research foundation of the Swiss Utilities.

ISP-42 was performed at the PANDA test facility - "Passive Nachwarmeabfuhr- und Druckabbau-Testanlage" ("Passive Decay Heat Removal and Depressurization Test Facility"), which had been constructed in Paul Scherrer Institute (PSI), Switzerland. The facility, as configured for the ISP-42 test, is a scaled down model of ESBWR containment and passive decay heat removal systems, with 1:40 volumetric and power scale, and is at full scale for elevations and time. The ISP-42 test was performed as a sequence of Phases A through F, representing typical passive safety system operating modes under standard or challenging conditions.

This paper presents results of blind and open calculations of ISP-42, performed with the SPECTRA computer code, and comparison with experimental data. Section 2 gives a short description of ISP-42. More detailed description may be found in [Aubert, 1999], [Lubb, 1999]. A short description of the SPECTRA [Stem, 1999a] model of PANDA facility is given in section 3. Results of calculations are compared to the experimental data in section 4. Summary and conclusions are given in section 5.

2 ISP-42

2.1 PANDA Test Facility

PANDA is a large scale facility, which has been constructed at Paul Scherrer Institute (PSI) for the investigation of both dynamic response and the key phenomena of passive containment systems during the long term heat removal phase for Advanced Light Water Reactors [Lubb, 1999]. The facility is a scaled down model of ESBWR containment and safety systems (figure 1), with 1:40 volumetric and power scale, and is at full scale for time and thermodynamic state.

The test facility consists of six large vessels: one representing RPV, two representing drywell, two representing wetwell, and one representing GDCS (Gravity Driven Cooling System) tank. The RPV contains a 1.5 MW electrical heat source. In the upper part of the facility there are four pools. One of the pools contains the IC (Isolation Condenser) unit, three others contain the PCC (Passive Containment Cooling) units. A PCC unit is a heat exchanger with vertical tubes. The unit consists of cylindrical upper drum, called also the steam box, twenty vertical tubes, and cylindrical lower drum, called also the water box. While the IC is connected to the RPV, the three PCC units are connected to the two drywell volumes. Two units are connected to one drywell, the third unit is connected to the other drywell.

2.2 Description of ISP-42

The ISP-42 test, performed in the PANDA facility, consists of six different phases, called Phase A, through F. Each of those phases is in fact a separate experiment, with its own initial and boundary conditions, specified in the ISP-42 documentation [Aubert, 1999]. ISP-42 consists of the following test phases:

- *Phase A: Passive Containment Cooling System Start-up.*
- *Phase B: Gravity Driven Cooling System Discharge.*
- *Phase C: Long Term Passive Decay Heat Removal.*
- *Phase D: Overload at Pure Steam Conditions.*
- *Phase E: Release of Hidden Air.*
- *Phase F: Release of Light Gas in Reactor Pressure Vessel.*

Description of the test phases, initial and boundary conditions, history of events, operator actions, etc., is provided in [Aubert, 1999].

3 SPECTRA MODEL

The model of PANDA facility used for both blind [Stem, 1999b] and open calculation is described in this section. Since facility configuration for the Phase F was much simpler than for all other phases, also a simpler SPECTRA model has been used for this case. The model used for simulation of Phases A through E is discussed in section 3.1. The model used for simulation of Phase F is discussed in section 3.2.

3.1 Model for Simulation of Phases A Through E

3.1.1 Model Applied for Blind Calculations

SPECTRA model of PANDA facility has been prepared based on data and drawings in [Lubb, 1999] and the MELCOR model of PANDA, used for simulation of PANDA P-series tests within the TEPSS project [Hart, 1998]. The nodalization is similar to that applied in MELCOR calculations.

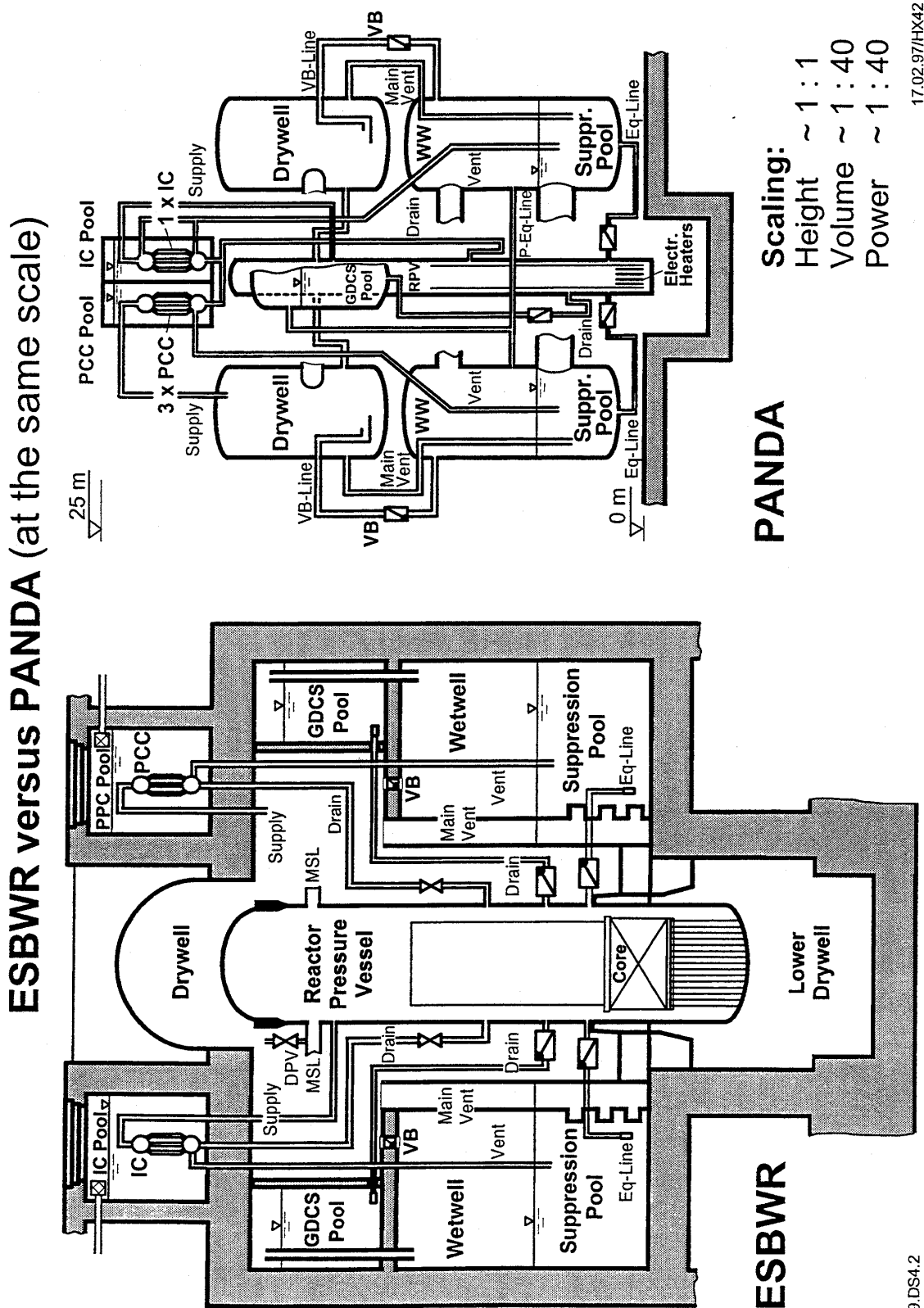


Figure 1 ESBWR versus PANDA test facility.

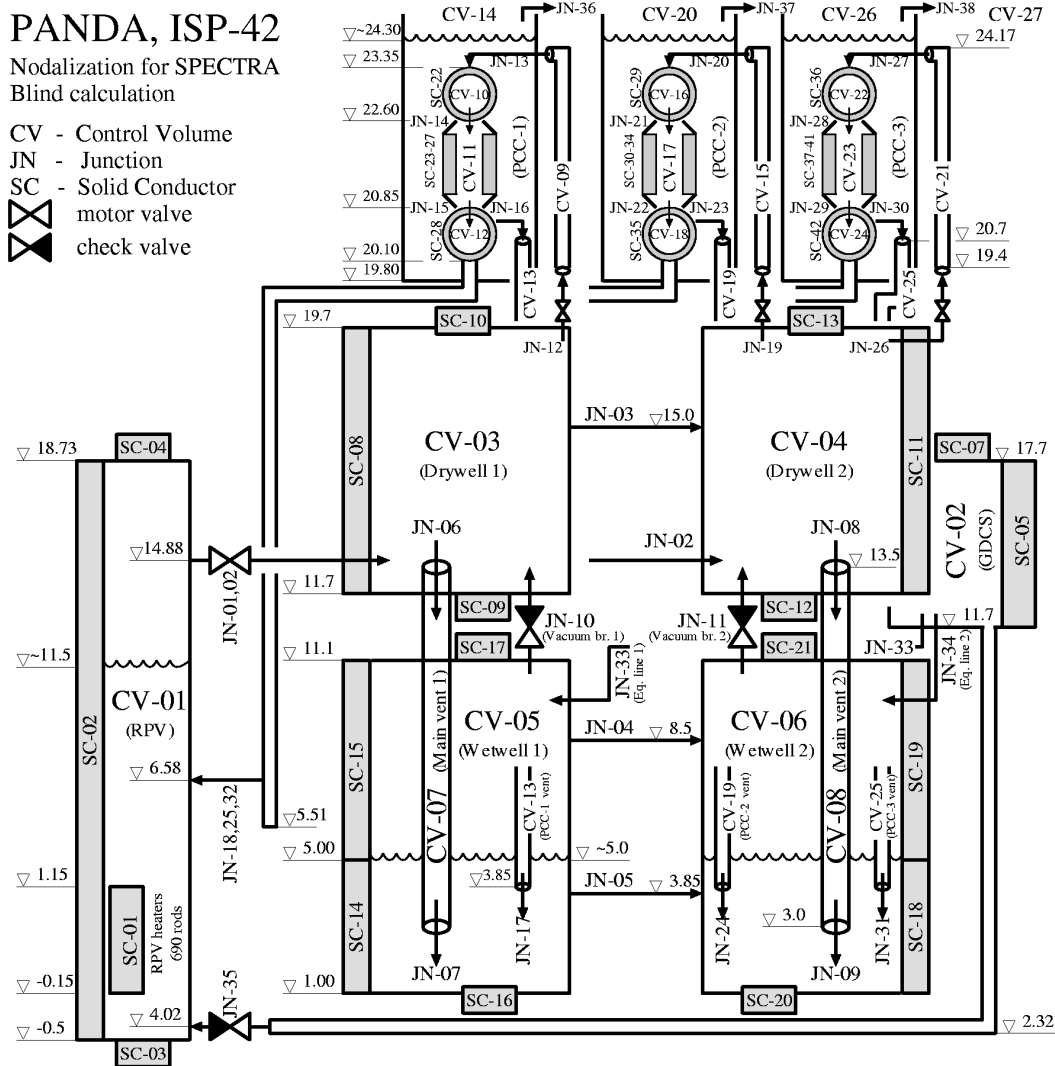


Figure 2
 SPECTRA model of PANDA test facility applied for test phases A through E, blind calculations.

The SPECTRA model is shown in figure 2. The model consists of 27 Control Volumes (CV), 38 CV Junctions (JN), eight of which are Valves (5 Motor Valves, 3 Check Valves), and 42 Solid Heat Conductors (SC). Note that PCC tubes are represented by five vertically stacked SC's, but only one CV. This has been changed in the open calculation.

Stratification models are enabled in the wetwell pools (pools of CV-05 and CV-06). Plume models are activated for all vents, that means two main vents (JN-07 and JN-08) and three PCC vents (JN-17, JN-24, JN-31).

For those test phases in which venting occurs to only one wetwell pool (Phases D, E, and F), the water line connecting the wetwells have been modelled using two junctions instead of one: the lower half represented by JN-005 and the upper half, represented by JN-039. This was done to allow mixing of warm water at the pool surface.

3.1.2 Modifications for Open Calculations

To perform open calculations several modifications were made in the model. The nodalization applied for open analysis is shown in figure 3. The model consists of 39 Control Volumes (CV), 50 CV Junctions (JN), eight of which are Valves (5 Motor Valves, 3 Check Valves), and 48 Solid Heat Conductors (SC). A full list of modifications made to perform open calculation is presented below.

- **Modification (1):** *Division of RPV walls into lower (water) and upper (steam) parts*
 In the model applied for blind calculations, RPV vertical walls were represented by a single 1D heat conductor (SC-002 - figure 2). Consequently, both water and steam in RPV were in contact with the same SC surface. This had no adverse effects for all phases, except for the Phase B. In Phase B cold water injected from GDCS quickly cooled down the RPV walls. In such circumstance steam condensation, occurring on the part of SC-002 above water surface, was significantly overpredicted (section 4.2, figure B.1). For open calculation SC-002 has been divided into two parts; the lower part, in contact with water (SC-002 - figure 3), and the upper part, in contact with atmosphere (SC-003 - figure 3).
- **Modification (2):** *Division of PCC primary side tube space into five CV's*
 In blind calculations PCC tube space was represented by a single CV. It was found out during the analysis of PCC steady state tests [Stem, 2000a] that a better representation is obtained by dividing PCC tubes into a number of connected CVs. For open analysis the PCC tubes were divided into five CVs (figure 4). With the revised nodalization the accumulation of air in the lower part of PCCs in Phase C was better represented (section 4.3, figures C.9, C.10), but the effect of this renodalization on the global parameters was minor.
- **Modification (3):** *Correction of error in loss factor for PCC feed lines*
 The loss factor for PCC feed lines was incorrectly specified in blind calculation. While the overall loss factor in these lines is about 30 [Aubert, 1999], the values used in the input resulted in overall factor of about 2 (K-factor of 1.0 in JN-012 and JN-013). This has been corrected in open analysis. This input error had the most clear consequences in Phase D. With small loss factor gas was pushed only through PCC vents, and the main vents were never cleared. In reality, as well as in open analysis, the large resistance of the PCC lines resulted in build up of pressure difference to a value sufficient to clear the main vents. Consequently the flow of gas into PCCs was much smaller (section 4.4, figures D.9, D.10).
- **Modification (4):** *Division of air lines into lower and upper halves*
 In relatively large pipes connecting drywells and wetwells (figure 1), counter-current flow and mixing of fluid may occur. This has been foreseen for wetwell water connecting line, and this line was modelled by two junctions for phases where pools were heated non-symmetrically (Phases D, E). It turned out that also in case of gas connecting lines the effect may be important. It was clearly seen in Phase E, where the air trapped in drywell 1 was slowly released to drywell 2; an effect that couldn't be captured with the connecting line modelled with only one junction (section 4.5, figure E.3). To improve prediction, the gas lines were divided into the lower and the upper halves for phase E.
- **Modification (5):** *Correction of initial conditions in PCC units*
 The initial conditions inside the PCC tubes, drums and piping system, were not given in the test specification. In absence of this data the relative humidity in these volumes were assumed equal to 0.9. Investigation of test results showed that for most phases an initial humidity of 1.0 was a better value. This value was applied in open analysis.

- Modification (6):** *Correction of initial air pressures indrywells*
 In some cases the initial air pressures given in test specification were not consistent with the initial gas temperatures. SPECTRA requires gas relative humidity as input parameter. The lowest possible noncondensable gas pressure in a Control Volume is obtained by setting the relative humidity to 1.0. In several cases even with humidity equal to 1.0 the initial air pressure in SPECTRA was higher than that given in the test specification. For the open analysis it was decided to adjust the initial gas temperatures, in order to obtain correct initial air pressures. This modification was important for Phase B (section 4.2, fig. B.3, B.4), and C (section 4.3, fig. C.3, C.4). The modifications of initial gas temperatures are listed below:

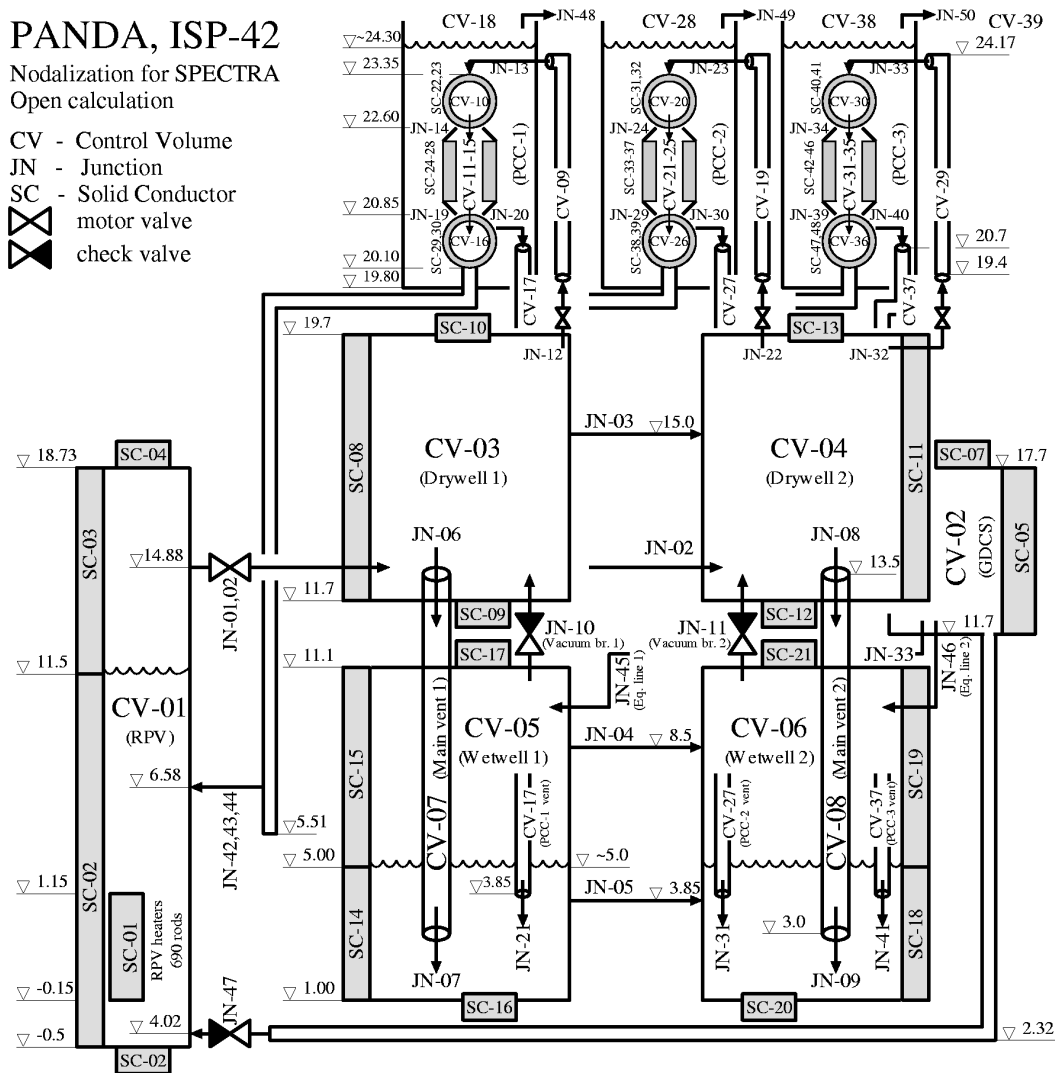


Figure 3
 SPECTRA model of PANDA test facility applied for test phases A through E, open calculations.

PANDA, ISP-42

Nodalization of PCC unit
Open calculation

CV - Control Volume
JN - Junction
SC - Solid Conductor

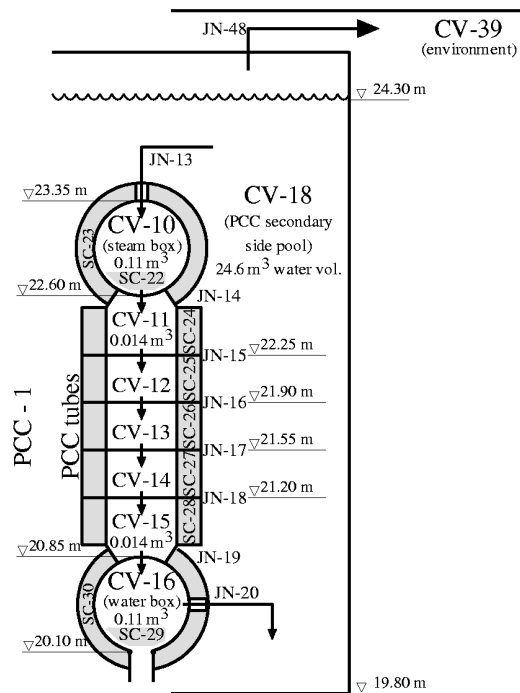


Figure 4
Nodalization of PCC unit applied for open calculations.

	Drywell 1	Drywell 2
Phase B:	+1.0 K	-
Phase C:	+1.5 K	-
Phase D:	+0.3 K	+0.4 K
Phase E:	+0.6 K	+0.4 K
Phase F:	+2.0 K	-

3.2 Model for Simulation of Phase F



3.2.1 Model Applied for Blind Calculations

The model applied for calculation of Phases F is shown in figure 5. Only the main vessels: RPV, DW1, DW2, GDCS, WW1, WW2, and only one vent pipe (from DW1 to WW1) were included in the model. The SPECTRA model for Phase F consists of seven Control Volumes, nine CV Junctions, two of which are Valves, and twenty one 1D Solid Heat Conductors. Gas stratification model has been activated in RPV.

It was intended to activate gas stratification model also in the drywells, but due to a mistake this has not been done. This mistake had a significant effect on the blind prediction (section 4.6).

PANDA, ISP-42, Phase F

Nodalization for SPECTRA

CV - Control Volume
 JN - Junction
 SC - Solid Conductor
 Valve
 He source

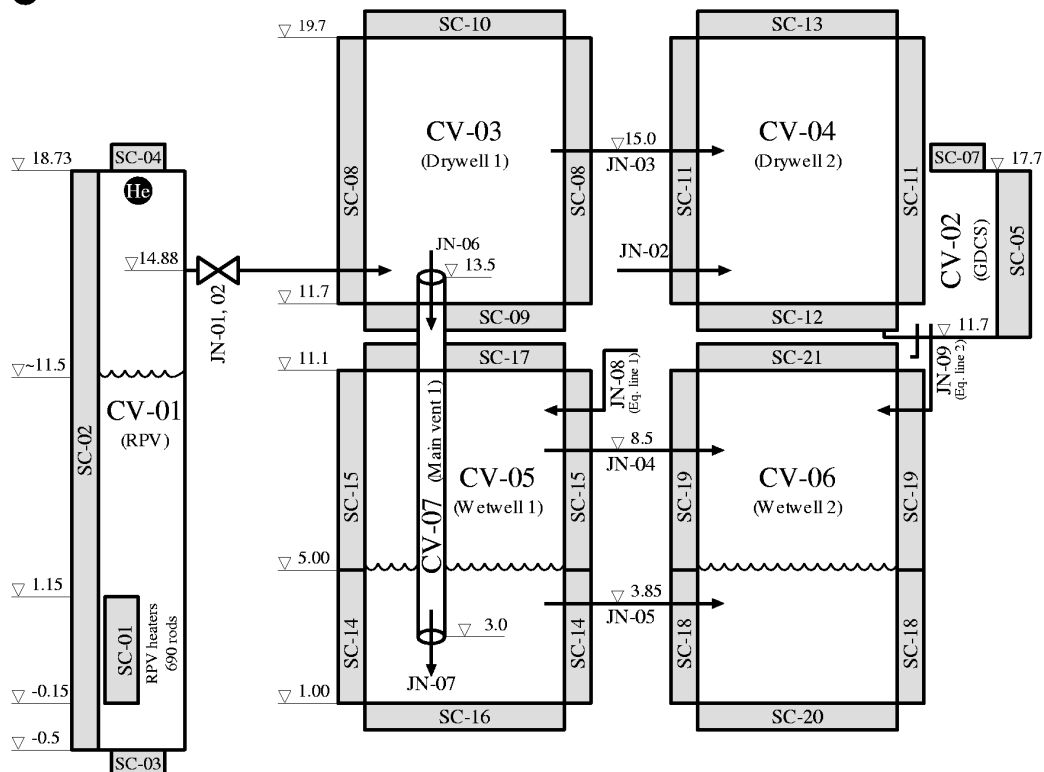


Figure 5
 SPECTRA model of PANDA test facility applied for test phase F,
 blind and open calculations.

3.2.2 Modifications for Open Calculations

Apart from the modification of the initial gas temperature in drywell 1, mentioned in section 3.1.2 (**Modification (6)** in section 3.1.2), the following three modifications were made for the open calculation of Phase F:

- **Modification (1):** *Division of air lines into lower and upper halves*
 The air lines between the drywells and the wetwells have been divided into the lower and the upper parts. This had to be done to capture mixing of different gases residing in different vessels (section 4.6, figures F.5, F.6).

- Modification (2): Gas stratification model in the drywell**

The gas density stratification model was activated in the drywells. SPECTRA offers several options to calculate density and thermal stratification of gas, as well as thermal stratification of pools. The gas density stratification model applied for phase F simulation may be shortly described as follows. Light gas (helium) entering a control volume is assumed to rise into the upper part of the volume and create a stratified layer there. If the steam saturation limit is not exceeded then the gas is allowed to create a perfectly stratified layer at the top of CV. The steam saturation limit is imposed to prevent from obtaining locally subcooled steam (local steam pressure exceeding saturation pressure). Other options are available in the code, density stratification may linked with thermal stratification, but these options were not used for phase F, since no significant thermal stratification in the drywells was expected. The stratification model had an important effect on the results of Phase F calculation (section 4.6, figures F.1, F.2).
- Modification (3): Initial thermal stratification of wetwell pools**

In blind calculations wetwell pool temperatures were initialized at constant temperatures, equal to the average pool temperature. In Phase F there was a small initial thermal stratification, which resulted in the fact that pool surface temperature was about 2 K higher than in SPECTRA. For open analysis the initial pool stratification has been taken into account, and the initial pool surface temperature was closer to the test data (section 4.6, figures F.11, F.12).

4 RESULTS

Results of blind and open calculations are compared to the measured data below, in sections 4.1 through 4.6, for the test Phases A through F respectively.

4.1 Phase A: Passive Containment Cooling System Start Up

For phase A results of blind calculation are in very good agreement with the experimental measurements [Lubb, 2000]. The modifications made for open calculation made almost no difference in the results, as may be seen by comparing figures A.1 and A.2

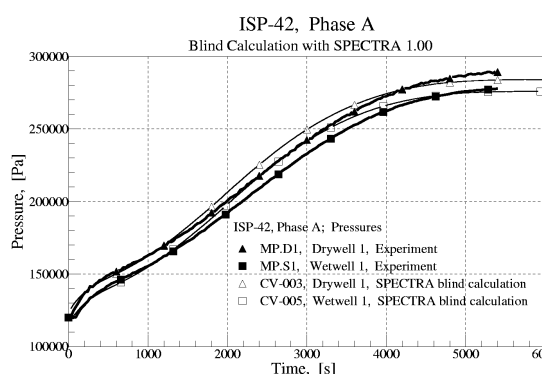


Figure A.1
Containment pressures, Phase A,
results of blind calculation versus experiment.

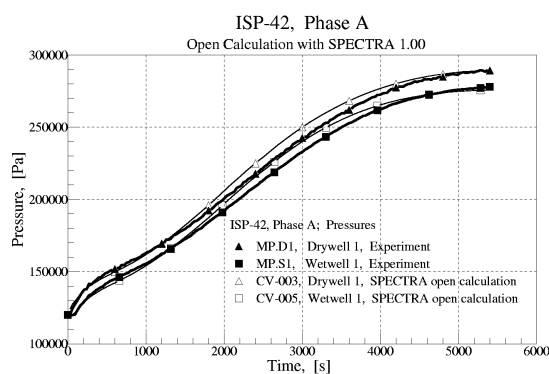


Figure A.2
Containment pressures, Phase A,
results of open calculation versus experiment.

4.2 Phase B: Gravity Driven Cooling System Discharge

GDCS injection starts at the beginning of the phase and lasts for about 1000 s (figures B.7, B.8). Due to the GDCS injection containment pressure decreases. In the blind calculation this pressure decrease was overestimated (figure B.1) because RPV walls were modelled by a single 1D Solid Heat Conductor (SC-002), which was in contact with both pool and atmosphere of CV. The temperature of the surface of SC-002 was very close to the temperature of RPV water, and intensive condensation took place on the part of SC-002 in contact with CV atmosphere. For open calculation the RPV walls were represented by two SCs - see section 3.1.2, **Modification (1)**. As a result of this change, the calculated pressures are in much better agreement with experiment during the GDCS injection phase (figure B.2).

The drywell gas composition was specified for blind calculation as 100% humid gas at temperature given by test specification. This resulted in too large initial air pressure in drywell 1. For the open analysis the initial air pressure in drywell 1 was corrected by increasing the initial gas temperature by 1.0 K - see section 3.1.2, **Modification (6)**. This improved the general agreement of calculated results with experiment (figures B.3, B.4, B.5, B.6).

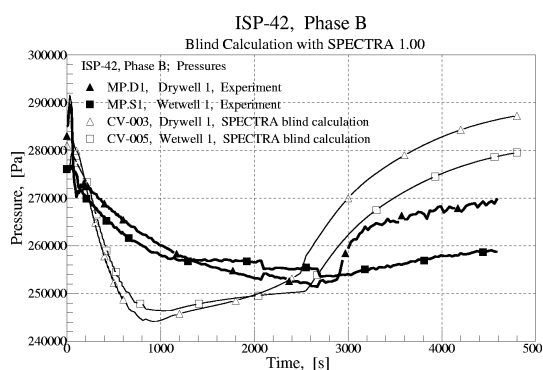


Figure B.1
Containment pressures, Phase B,
results of blind calculation versus experiment.

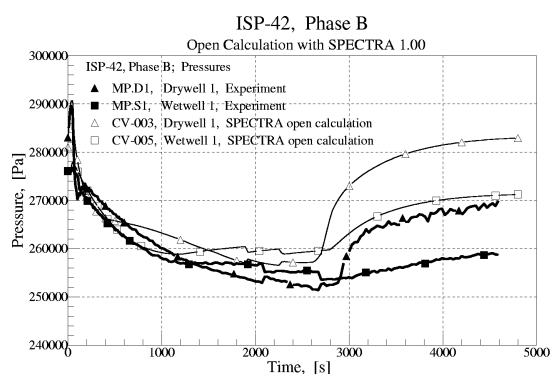


Figure B.2
Containment pressures, Phase B,
results of open calculation versus experiment.

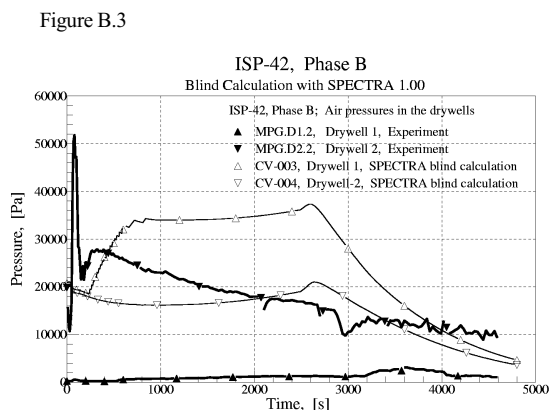


Figure B.3
Air pressures in the drywells, Phase B,
results of blind calculation versus experiment.

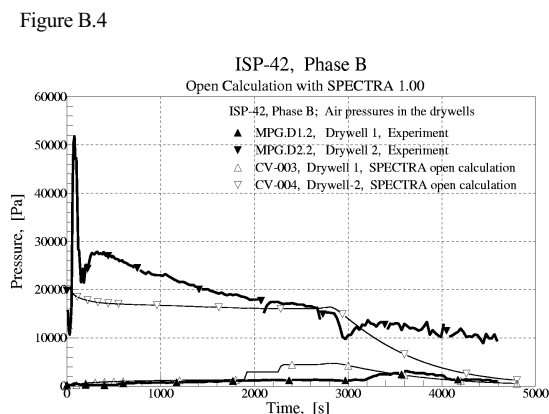


Figure B.4
Air pressures in the drywells, Phase B,
results of open calculation versus experiment.

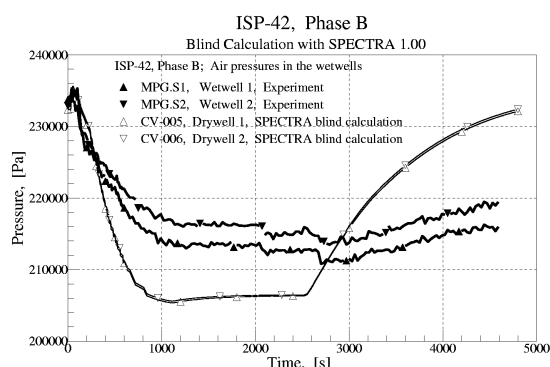


Figure B.5
Air pressures in the wetwells, Phase B,
results of blind calculation versus experiment.

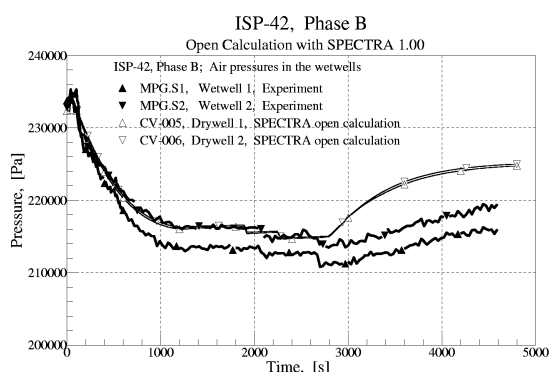


Figure B.6
Air pressures in the wetwells, Phase B,
results of open calculation versus experiment

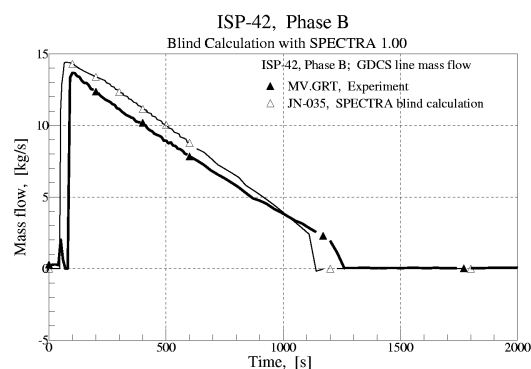


Figure B.7
GDCS flow, Phase B,
results of blind calculation versus experiment.

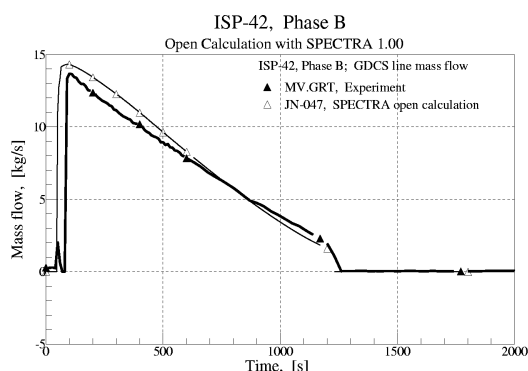


Figure B.8
GDCS flow, Phase B,
results of open calculation versus experiment.

4.3 Phase C: Long Term Passive Decay Heat Removal

Results obtained for Phase C are shown in figures C.1 - C.10. Generally quite good agreement was obtained already in blind calculation. Containment pressure was slightly overpredicted (figure C.1). For the post test analysis two modifications of the model, discussed below, had an important effect on the Phase C results.

Firstly, in the open analysis the PCC tubes were modelled by five connected CVs, instead of one CV - see section 3.1.2, **Modification (2)**. This modification allowed to represent better the gas composition change in the tubes, namely the accumulation of air in the lower part of the PCC tubes. This accumulation is visible in figure C.9, showing the temperature difference between the primary and the secondary side of the PCC units. In the second half of the test the temperature difference becomes small, which means that steam is condensed, and a relatively cold air fills the tubes. In the blind calculation this effect couldn't be captured, because steam concentration was constant along the tubes. Consequently, the calculated temperature difference was large during the whole test (figure C.9), and

approximately the same for all SCs representing the tubes. In the open calculation the temperature difference for lower SCs becomes small in the second half of the test (figure C.10).

It is seen in figure C.10 that the temperature difference similar to that measured at the elevation of the middle point of PCC tubes (measurement MTG.P1.7, MTL.U1.4) is observed for the Solid Heat Conductor SC-027, that means in calculations the accumulation of air occurs slightly lower than in the test. This could possibly be improved by dividing PCC tubes into larger number of CVs and SCs. The division of PCC tubes into five CVs allowed to improve the agreement of the PCC temperature difference, but had almost no effect on the overall parameters, like for example the containment pressure, which, with this modification alone, were practically identical as in the blind analysis. To improve the pressure prediction the modification described below was needed.

Secondly, the initial air pressures in the drywells were corrected by increasing slightly the initial gas temperatures - see section 3.1.2, **Modification (6)**. This improved the containment pressure prediction (figure C.2). As in Phase B, some air remained trapped in the lower part of the drywell 2 (figure C.3), an effect that couldn't be captured in the calculations. In order to improve the prediction in that respect, a detailed 3D model of the drywell should be made, which will be possible when a "CFD module" is implemented into the code, which is planned to do in the near future.

It is seen in figures C.1 and C.2 that in the open analysis the pressure difference between the drywell and the wetwell is somewhat larger than in the blind calculation. This is a consequence of correcting the loss factors for the PCC feed lines - see section 3.1.2, **Modification (3)**. The error in the feed lines loss factor did not have very important effect on the overall system performance, since PCC units were only partly loaded in this case. All steam coming into the PCC feed lines (figures C.5, C.6) was condensed (figures C.7, C.8). In the Phase D, where PCC were overloaded, this error had more important consequences (see section 4.4 below).

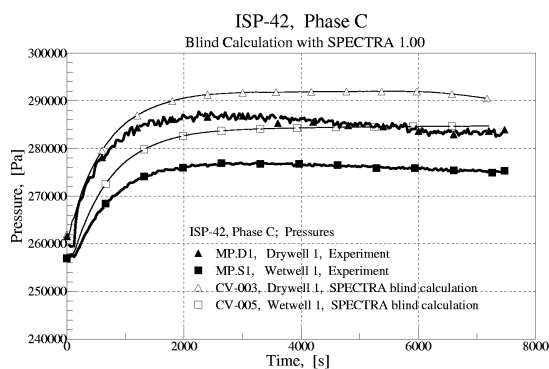


Figure C.1
Containment pressures, Phase C,
results of blind calculation versus experiment.

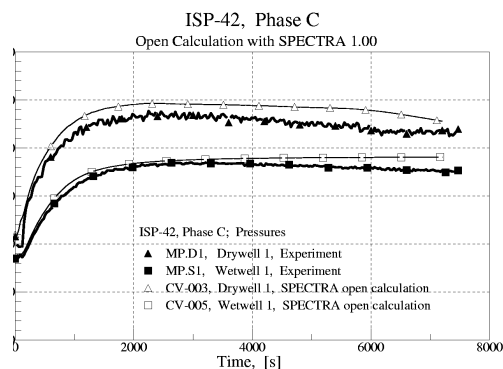


Figure C.2
Containment pressures, Phase C,
results of open calculation versus experiment.

Analysis of ISP-42, PANDA Test, with the SPECTRA Code

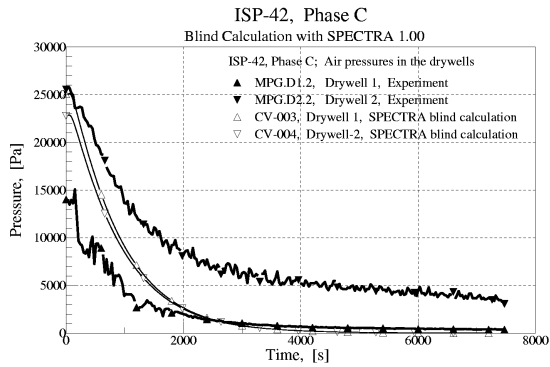


Figure C.3
Air pressures in the drywells, Phase C,
results of blind calculation versus experiment.

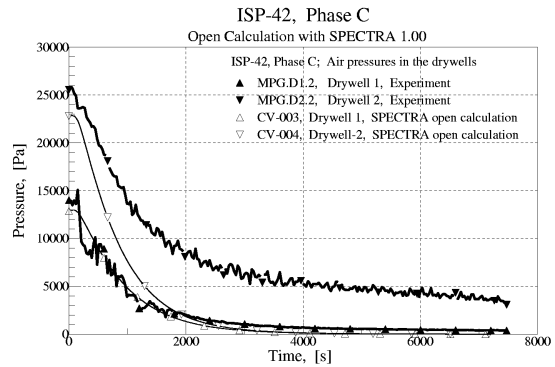


Figure C.4
Air pressures in the drywells, Phase C,
results of open calculation versus experiment.

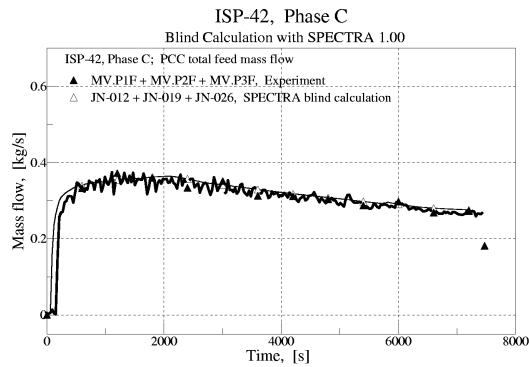


Figure C.5
PCC total feed flow, Phase C,
results of blind calculation versus experiment.

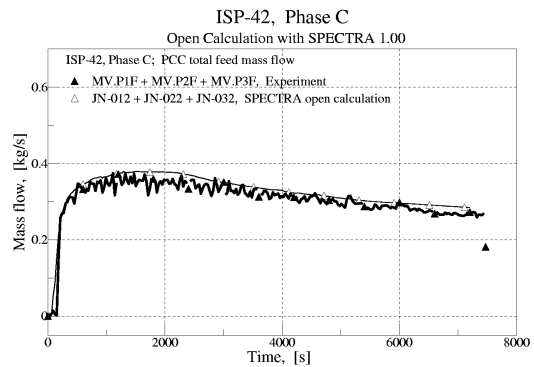


Figure C.6
PCC total feed flow, Phase C,
results of open calculation versus experiment.

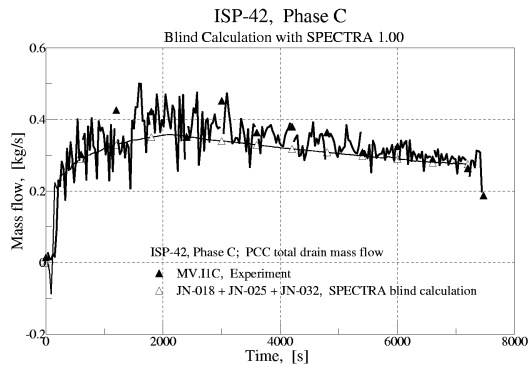


Figure C.7
PCC total drain flow, Phase C,
results of blind calculation versus experiment.

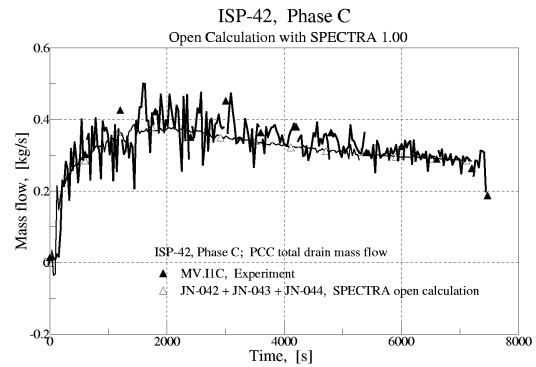


Figure C.8
PCC total drain flow, Phase C,
results of open calculation versus experiment.

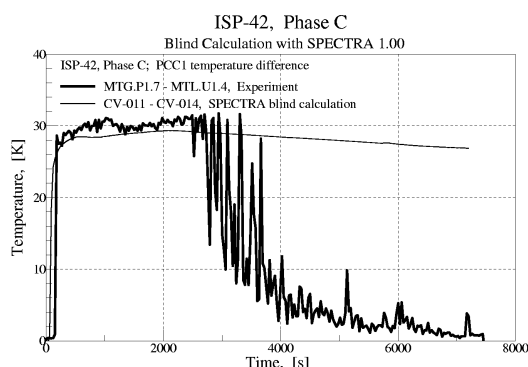


Figure C.9
PCC temperature difference, Phase C,
results of blind calculation versus experiment.

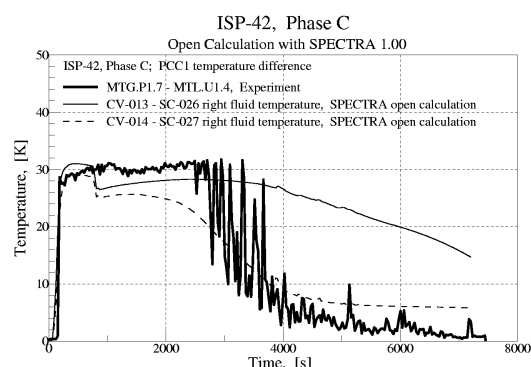


Figure C.10
PCC temperature difference, Phase C,
results of open calculation versus experiment.

4.4 Phase D: Overload at Pure Steam Conditions

Phase D is the only phase of ISP-42 for which for some parameters the open calculation seem to give worse agreement with experiment than the blind calculation (figures D.1, D.2). During Phase D the two operating PCC units (both on drywell 2) were overloaded. The excess of steam, which couldn't be condensed in PCCs, was vented to the wetwell pools, rising the pool surface temperature. This caused an increase of the steam partial pressure in the wetwells (usually close to the saturation pressure at the pool surface temperature), and consequently an increase of the total containment pressures.

For Phase D, the most important modification made for the open analysis was the correction of the PCC feed lines loss factor - section 3.1.2, **Modification (3)**. In the blind calculation the resistance of the PCC feed lines was too low (loss factor of ~ 2 instead of ~ 30). As a consequence, the uncondensed steam was vented through the PCC vents, rather than the main vents. This is seen in figure D.9, as all steam coming from RPV (figure D.7) was entering the PCC units. Due to too low loss factor, the pressure difference between drywells and wetwells could not build up sufficiently to clear the main vents. In the open calculation the loss factor was correct, and the calculated mass flow through PCC units was in very good agreement with experiment (figure D.10). The excess of steam was vented through the main vent pipes.

Because in open calculation the main vents were cleared, the gas was flowing through the drywell 1, which in the blind analysis remained a "dead-end" volume with approximately constant air content (figure D.3). In open analysis the gas flow through drywell 1 slowly pushed the air from this vessel to the wetwells (figure D.4). This fact caused an increased wetwell pressure in open calculation, and worsened the wetwell pressure prediction, compared to the blind calculation. Note that for the open analysis the initial air pressures in the drywells were adjusted to agree better with measured values (figures D.3, D.4) - see section 3.1.2, **Modification (6)**. If this hadn't been done, the wetwell pressure in the open analysis would have been even higher.

Analysis of ISP-42, PANDA Test, with the SPECTRA Code

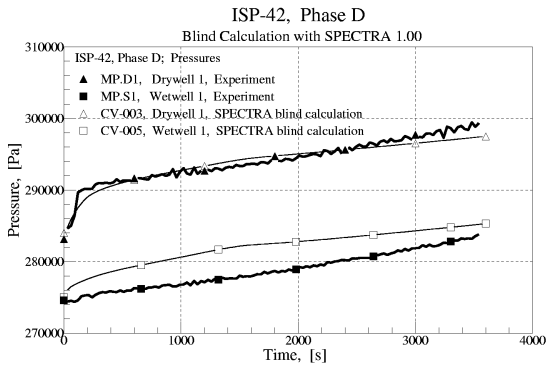


Figure D.1
Containment pressures, Phase D,
results of blind calculation versus experiment.

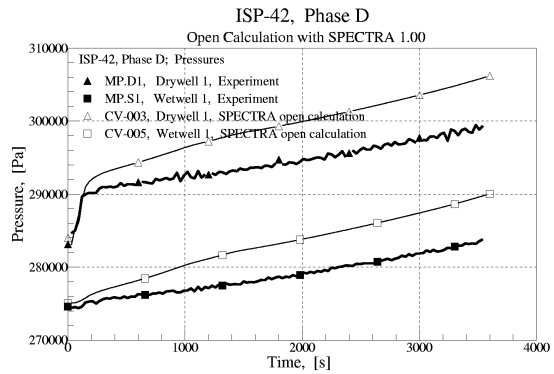


Figure D.2
Containment pressures, Phase D,
results of open calculation versus experiment.

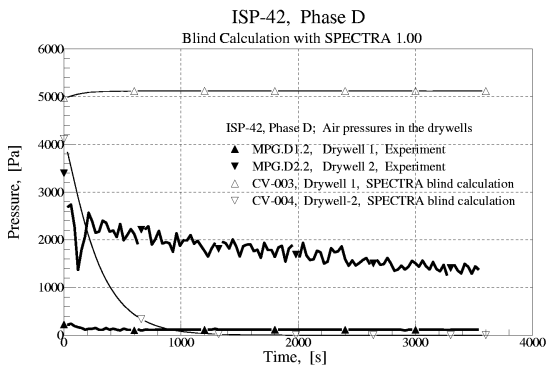


Figure D.3
Air pressures in the drywells, Phase D,
results of blind calculation versus experiment.

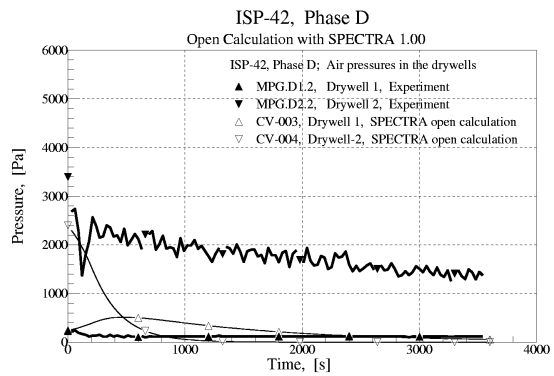


Figure D.4
Air pressures in the drywells, Phase D,
results of open calculation versus experiment.

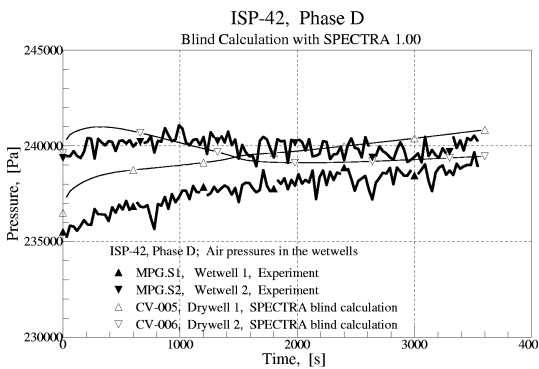


Figure D.5
Air pressures in the wetwells, Phase D,
results of blind calculation versus experiment.

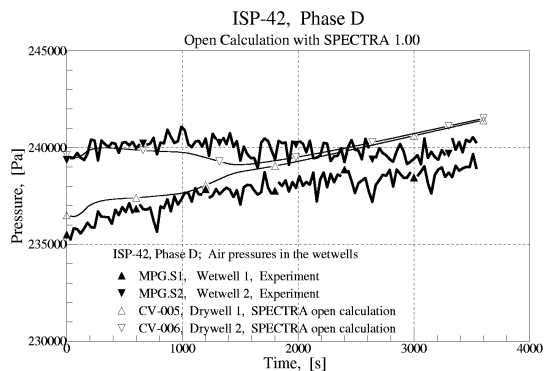


Figure D.6
Air pressures in the wetwells, Phase D,
results of open calculation versus experiment.

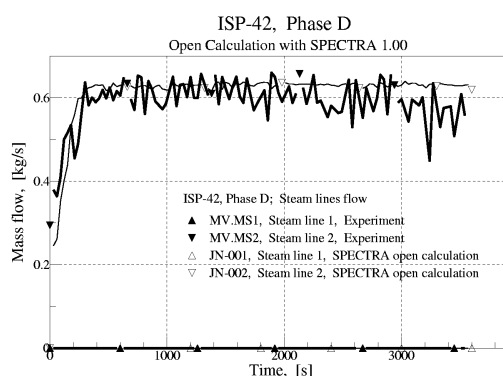


Figure D.7
Steam lines flow, Phase D,
results of blind calculation versus experiment.

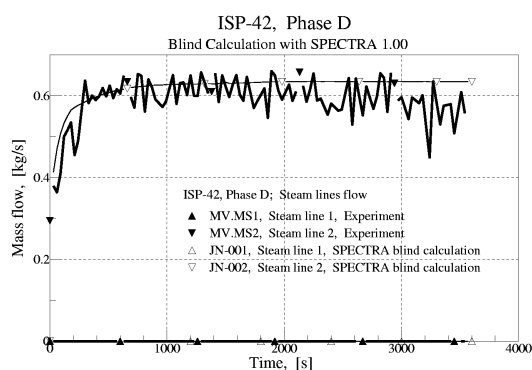


Figure D.8
Steam lines flow, Phase D,
results of open calculation versus experiment.

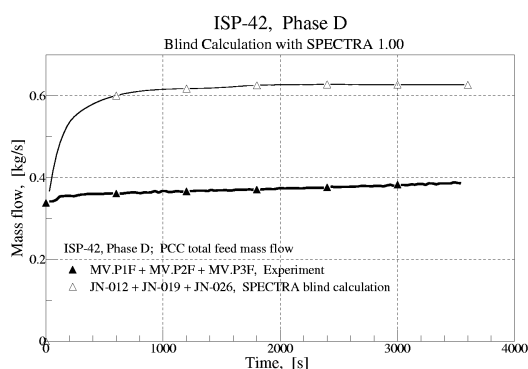


Figure D.9
PCC total feed flow, Phase D,
results of blind calculation versus experiment.

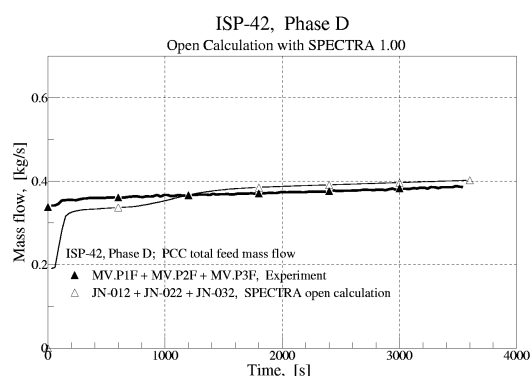


Figure D.10
PCC total feed flow, Phase D,
results of open calculation versus experiment.

4 Phase E: Release of Hidden Air

During the first half an hour of the test air was injected into the drywell 1. Since the PCC connected to drywell 1 was isolated in this phase, then, as long as the main vent is not cleared, the drywell 1 may be viewed as a "dead-end" volume. The blind simulation resulted in a clear underestimation of the containment pressure (figure E.1). This underestimation was caused by the fact that in the calculations the injected air stayed inside the "dead-end" drywell 1 vessel during the whole test (figure E.3). In the experiment however, the air from drywell 1 was entering the rest of the system, which is clearly seen in figure E.3. The reason for this discrepancy between the experiment and the blind calculation is twofold.

Firstly, in the experiment air-rich gas from drywell 1 was constantly mixing with steam-rich gas from drywell 2. As a result some small amounts of air were constantly entering drywell 2, and the two operating PCC units, where they were degrading the PCC performance. This phenomenon could not be captured in the blind calculation, because the line connecting drywells was represented by a single junction. For the open analysis the air line was divided into a lower and an upper half - see section

3.1.2, **Modification (4)**. With this division the gas mixing in the drywells was calculated quite well (figure E.4). The air entering drywell 2 was pushed through PCC and vented to the wetwell. This was also correctly calculated in the open analysis (figure E.6).

Secondly, the mistake in the resistance of the PCC feed line resulted in the fact that the main vents were never cleared (see also description of Phase D, section 4.4). The venting was performed through the vent lines of the two operating PCCs, rather than through the main vents. This had an additional contribution to the isolation of air in drywell 1 in the blind analysis.

The fact that all uncondensed gas was pushed through the PCC vents rather than the main vents is clearly seen in figures E.7, E.9. In the blind analysis the total mass flow through PCC units (figure E.9) is practically the same as the steam flow coming from RPV (figure E.7). In the open calculation, where the resistance of the PCC feed lines was corrected - see section 3.1.2, **Modification (3)**, only part of the incoming steam was pushed through the PCCS (figures E.8, E.10). The remaining steam was vented through the main vents, so both to wetwell 1 and 2.

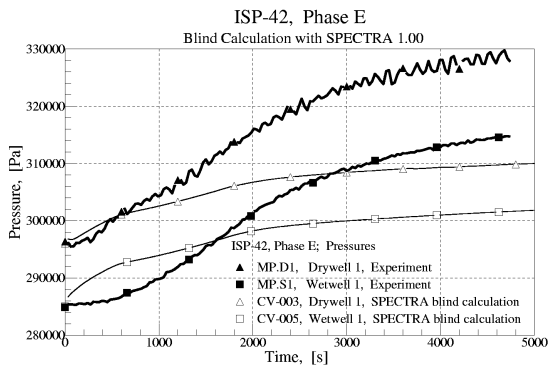


Figure E.1
Containment pressures, Phase E,
results of blind calculation versus experiment.

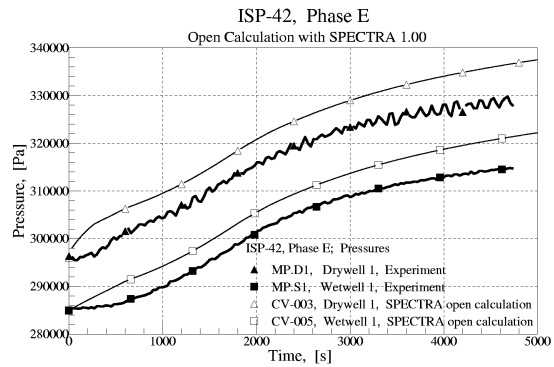


Figure E.2
Containment pressures, Phase E,
results of open calculation versus experiment.

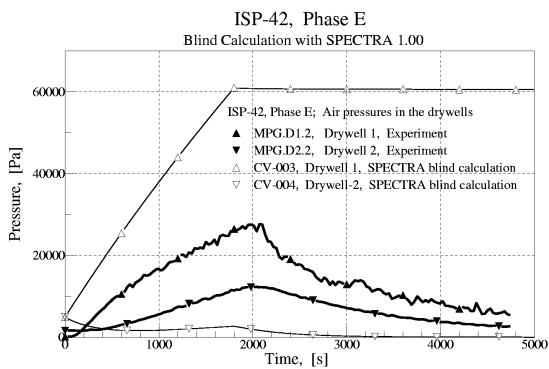


Figure E.3
Air pressures in the drywells, Phase E,
results of blind calculation versus experiment.

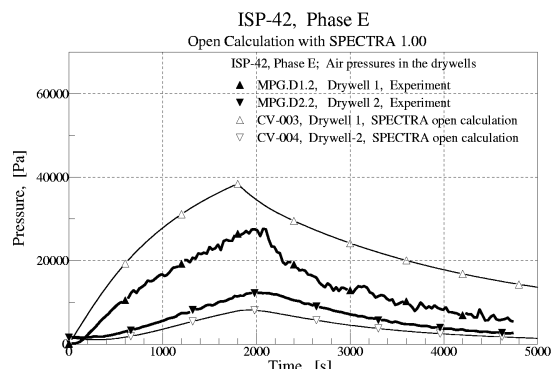


Figure E.4
Air pressures in the drywells, Phase E,
results of open calculation versus experiment.

Analysis of ISP-42, PANDA Test, with the SPECTRA Code

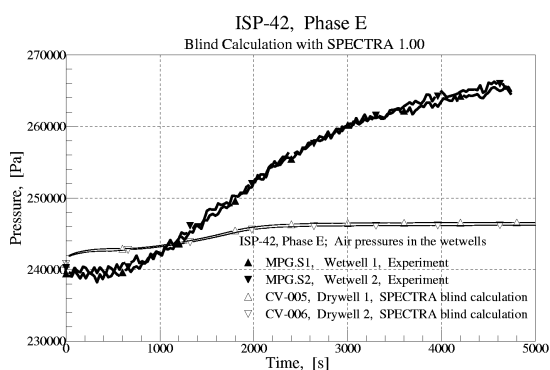


Figure E.5
Air pressures in the wetwells, Phase E,
results of blind calculation versus experiment.

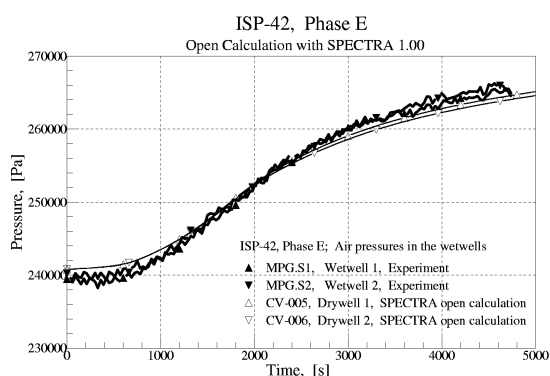


Figure E.6
Air pressures in the wetwells, Phase E,
results of open calculation versus experiment.

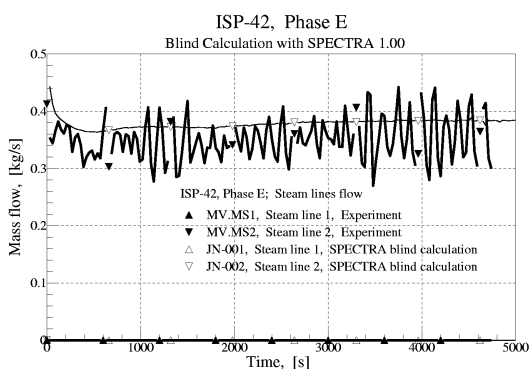


Figure E.7
Steam lines flow, Phase E,
results of blind calculation versus experiment.

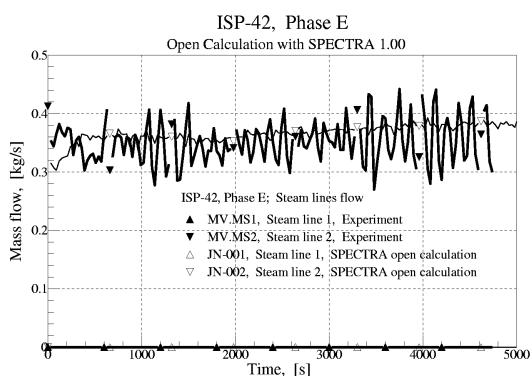


Figure E.8
Steam lines flow, Phase E,
results of open calculation versus experiment.

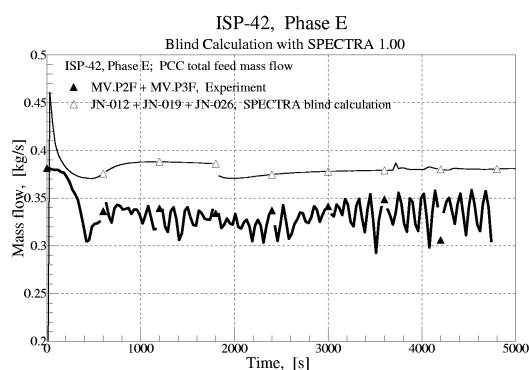


Figure E.9
PCC total feed flow, Phase E,
results of blind calculation versus experiment.

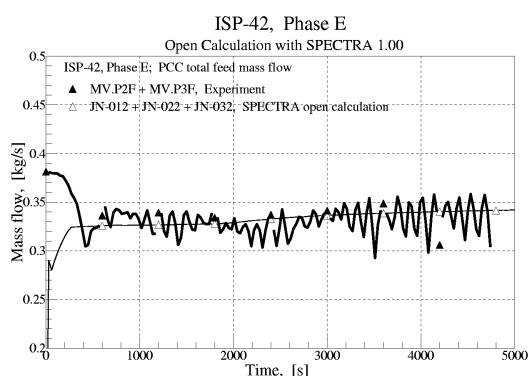


Figure E.10
PCC total feed flow, Phase E,
results of open calculation versus experiment.

4.6 Phase F: Release of Light Gas in Reactor Pressure Vessel

During Phase F helium was injected into the RPV during the time period between 900 s and 2700 s. Only one steam line (from RPV to drywell 2) and only one main vent pipe (from drywell 1 to wetwell 1) were open. All PCC units were isolated. The helium injected into RPV was flowing first into drywell 2, next to drywell 1, then it was vented into wetwell 1, and finally it mixed with the gas of wetwell 2. Results obtained for Phase F are shown in figures F.1 - F.14.

In the blind analysis the containment pressure was overestimated (figure F.1). The main reason for this overestimation was the lack of gas density stratification model in the drywells. When the stratification model was activated in the drywells - see section 3.2.2, **Modification (2)** - the calculated containment pressures were in very good agreement with experiment (figure F.2). With the stratification model the air is trapped in the lower part of the drywells and some amount of air remains in the drywells. It is seen in figure F.4 that air remains in both drywells.

Another indication of the presence of gas stratification in the drywells is the behavior of water mass in the drywells (figures F.9, F.10). In the blind analysis a decrease of water mass in the drywells was calculated in the period between ~1200 s and ~3500 s. This decrease was caused by evaporation of water into a relatively dry atmosphere above the surface of the water pools in the drywells. The atmosphere was dry because of large amount of helium present in this period in the drywells. This evaporation however was not observed in the experiment! This means that in the experiment the gas above the pool surface was humid, which in turn means that helium was concentrated in the upper parts of the drywells. In the open calculation, with the stratification model in the drywells, the water mass in the drywells was increasing (figure F.10), similarly as in experiment, although the increase was somewhat slower.

Correction of initial air pressure in drywell 1 - see section 3.1.2, **Modification (6)** - allowed to obtain better agreement of air partial pressures with experiment (figures F.3, F.4). Division of air lines into a lower and an upper half - see section 3.2.2, **Modification (1)** - allowed to better represent the gas mixing, specifically in the wetwells (figures F.5, F.6).

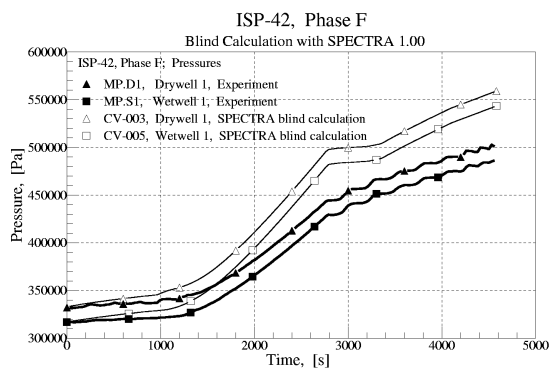


Figure F.1
Containment pressures, Phase F,
results of blind calculation versus experiment.

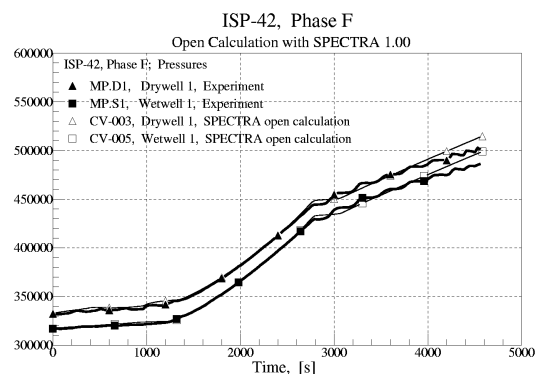


Figure F.2
Containment pressures, Phase F,
results of open calculation versus experiment.

Analysis of ISP-42, PANDA Test, with the SPECTRA Code

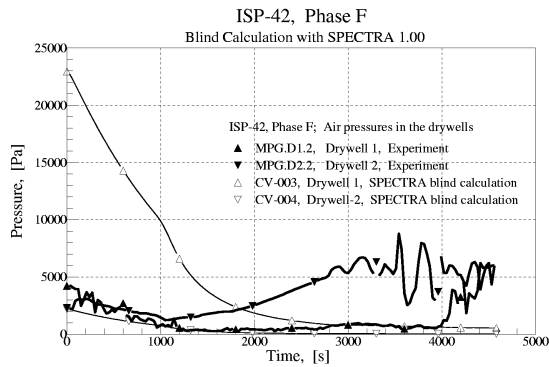


Figure F.3
Air pressures in the drywells, Phase F,
results of blind calculation versus experiment.

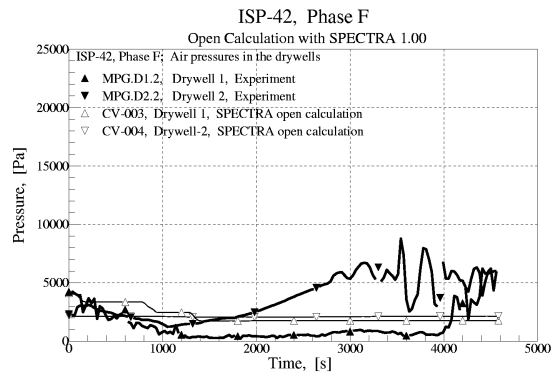


Figure F.4
Air pressures in the drywells, Phase F,
results of open calculation versus experiment.

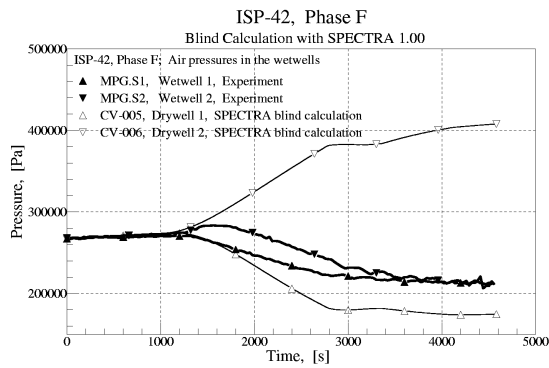


Figure F.5
Air pressures in the wetwells, Phase F,
results of blind calculation versus experiment.

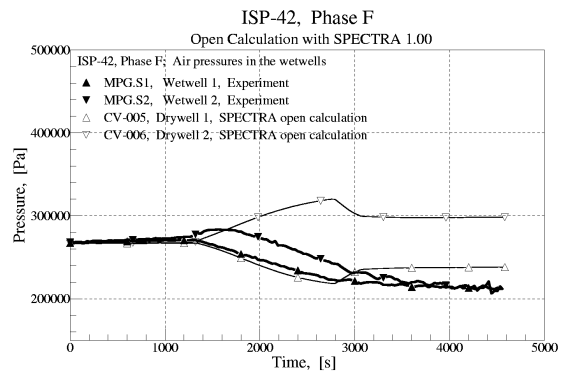


Figure F.6
Air pressures in the wetwells, Phase F,
results of open calculation versus experiment.

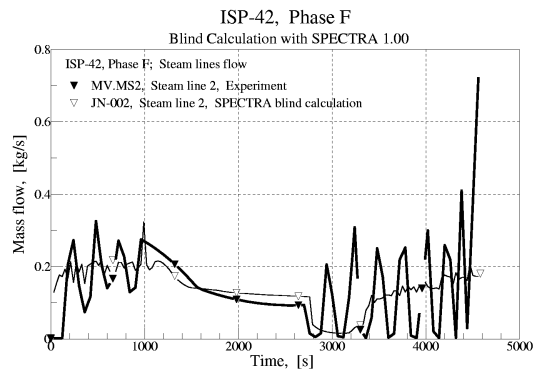


Figure F.7
Steam lines flow, Phase F,
results of blind calculation versus experiment.

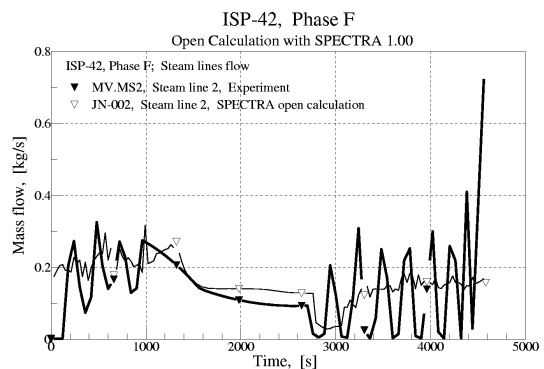


Figure F.8
Steam lines flow, Phase F,
results of open calculation versus experiment.

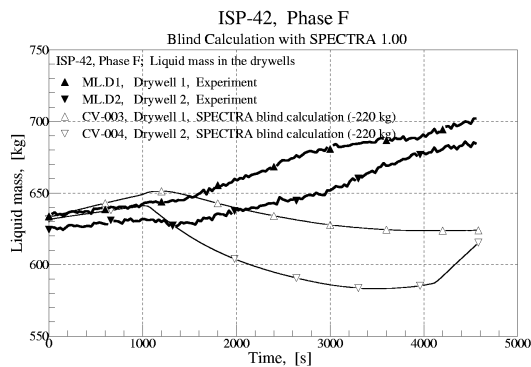


Figure F.9
Liquid mass in the drywells, Phase F,
results of blind calculation versus experiment.

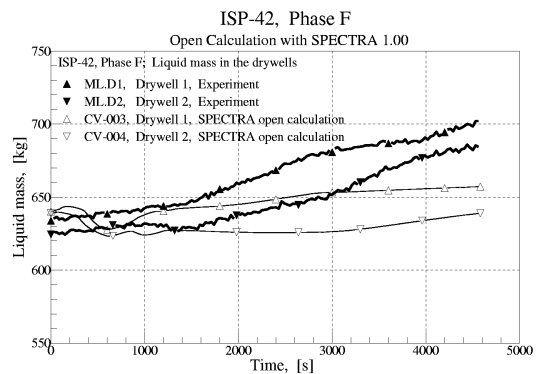


Figure F.10
Liquid mass in the drywells, Phase F,
results of open calculation versus experiment.

5 SUMMARY AND CONCLUSIONS

5.1 Summary

Blind and open calculations were performed for all six phases of ISP-42. Results obtained in blind calculations were in good agreement with experiment. For open analysis some input errors and modelling deficiencies were corrected. The main modifications made for the open analysis were correction of PCC feed lines loss factors, correction of the initial air pressures, and some nodalization changes. Results of the open calculations were generally closer to the experiment than the blind results. Results of blind and open calculations are summarized below for each phase of the ISP.

- For **Phase A** a very good blind prediction was obtained. According to the comparison made at PSI [Aksan, 2000], out of all blind calculations of ISP-42, SPECTRA provided results closest to the experiment for this phase. Results of the open calculations were almost identical as the blind results.
- For **Phase B** the discrepancies between blind results were caused mainly by using a single Solid Heat Conductor to represent the RPV walls. In the open analysis two Heat Conductors, one for the water covered part, and one for the steam part, were used. This resulted in significantly improved prediction for this test phase.
- For **Phase C** quite good agreement was obtained in the blind results. Open results provided better agreement with experiment, mainly because of correction of the initial air pressures in the drywell. Division of PCC tubes into five Control Volumes improved prediction of detailed results inside PCCs.
- For **Phase D** the most important modification made for the open analysis was the correction of the PCC feed lines loss factor. Correction of the loss factors resulted in good prediction of the division of flow between PCCs and main vents.
- For **Phase E** a relatively bad blind prediction was obtained. This was caused mainly by the fact that with the applied nodalization (single junction used to represent drywell air line), it was impossible to capture the mixing of the air-rich mixture from drywell 1 with the steam-rich mixture from drywell 2. In the open analysis the air line between drywells was represented by two junctions and the results were very close to the experiment.

- For **Phase F** too high containment pressure was obtained in the blind analysis. This trend was observed in all blind predictions [Lubb, 2000]. In open analysis a stratification model was activated in drywells, which resulted in helium being preferentially deposited in the upper part of the drywells. With this model an excellent agreement in containment pressures was obtained.

One general remark can be made related to all test phases.

- In **all test phases** some small accumulation of air in drywell 2 was observed. Most of the air residing initially in the lower part of the vessel, stayed there during the each test phase. This effect was not captured in calculations. To predict it a CFD module needs to be implemented into the SPECTRA code. Before the CFD module is implemented, SPECTRA may be used together with a CFD code, to perform a complementary analysis. The CFD code would in such case be used to model selected part of the system, for which detailed 3D analysis is needed. The CFD code would use SPECTRA preliminary results to determine necessary boundary conditions. Results of the CFD code would then be used in SPECTRA to perform final analysis, taking data from the CFD code and using the "manually controlled" stratification in the selected part of the system.

5.2 Conclusions

Based on the performed exercise several conclusions may be drawn.

- A user should avoid using long 1D heat conducting structures, that may be in contact with both pool and atmosphere of a Control Volume. This observation is expected to be valid not only for SPECTRA, but for all codes with similar concept of Control Volumes (relatively large CVs, with defined pool surface), that is CONTAIN, MELCOR, MAAP, RELAP4. It is not applicable for codes working with relatively small, homogeneous CVs, such as RELAP5, TRAC.
- A better representation of PCC tubes is obtained if they are divided into a number of Control Volumes. This is again expected to be valid for codes like CONTAIN, MELCOR, etc. With this representation a SPECTRA (CONTAIN, MELCOR) model of a PCC unit becomes more similar to a model used by RELAP5 or TRAC, where it is natural to divide tubes into a relatively large number of Control Volumes. There are no adverse effects caused by the fact that the code "thinks" that there are multiple pool surfaces inside the tubes. Care should be taken however that the drainage of condensate from one heat conductor to another is properly modelled. In codes like MELCOR and SPECTRA the condensate drainage model is present and may easily be applied for such case.
- In case of relatively large openings between vessels, such as the drywell air line as well as the wetwell air and water lines in PANDA, it is better to use two junctions (representing the lower part and the upper part of the opening respectively), rather than using a single junction. This modelling allows to capture mixing of different gases residing in different vessels, or mixing of water if the water pools are at different temperatures. This conclusion is expected to be valid independently of the code used, thus not only for SPECTRA, MELCOR, CONTAIN, but also TRAC, RELAP5, etc.
- Care should be taken that appropriate input parameters, for example loss coefficients, etc., are used in an analysis. To ensure this, every input model should be reviewed as carefully as possible. An important factor is the user's discipline. This discipline cannot be forced, or substituted, by QA procedures. This conclusion is of course independent of the code used.
- In cases when light gas is present in the analyzed system, the simple stratification models offered by

SPECTRA, may significantly improve results. In case when stratification problems are deemed specifically important in a selected part of the system, a complementary SPECTRA-CFD analysis may be performed, with a full system modelled with SPECTRA, and the selected part of the system modelled with CFD. This conclusion is SPECTRA specific.

References

- Aksan, 2000 N. Aksan, S. Bonato, "Quantifying the accuracy - an experiment adopting Fast Fourier Transform on the ISP-42", draft material, presented at the second workshop on ISP-42 PANDA tests, PSI, 5-7 July, 2000.
- Aubert, 1999 C. Aubert, J. Dreier, "ISP-42, PANDA Test Phases, History of Events, Boundary and Initial Conditions, Calculational Parameters", PSI report, TM-42-98-40, ALPHA-835-1, January 1999.
- Breitung, 2000 W. Breitung, et al., "Flame Acceleration and Deflagration-to-Detonation Transition in Nuclear Safety", NEA/CSNI/R(2000)7, October 2000.
- Hart, 1998 J. Hart, M. Stempniewicz, "Post Test Analysis of PANDA Test P7", INNO-TEPSS(98)-D17, NRG/PPT 30086-NUC 98-3104, December, 1988.
- Lubb, 1999 D. Lübbsmeyer, et al., "ISP-42, Description PANDA Test Facility", PSI report, TM-42-98-41, ALPHA-836-1, January 1999.
- Lubb, 2000 D. Lübbsmeyer, N.S. Aksan, "ISP-42 (PANDA) Blind Phase Comparison Report", PSI report, Draft version July 2000.
- Slootman, 1998 M.L.F. Slootman, M.M. Stempniewicz, "Analysis of International Standard Problem 29 by the Thermal-hydraulic Code SPECTRA, Part I - Description of Input Model; Part II - Results", KEMA report, Part I: 41458-NUC 97-2977, December 1997; Part II: 41458-NUC 98-2646, July 1998.
- Stem, 1999a M.M. Stempniewicz, "SPECTRA - Simplified Parametric Evaluation of Containment Transient Response during Accidents", Version 1.00, December 1999; Volume 1 - Description of Models; Volume 2 - User's Guide; Volume 3 - Description of Subroutines; Volume 4 - Verification", NRG report, 26094/99.52612/C, Arnhem 5 October 1999.
- Stem, 1999b M.M. Stempniewicz, "Analysis of ISP-42, PANDA Test, Blind Calculations with the SPECTRA Code", NRG report, 26098/99.52567, November 1999.
- Stem, 2000a M.M. Stempniewicz, "Simulation of Containment Transient Response During Accidents in Advanced Reactor Types - The Computer Code SPECTRA", PhD Thesis at Silesian Technical University, Gliwice, Poland, NRG report, 21437/00.52167/P, May 2000.
- Stem, 2000b M.M. Stempniewicz, "SPECTRA - Software for Profound Evaluation of Containment Transient Response during Accidents, Version 1.10, July 2000; Volume 1 - Program Description; Volume 2 - User's Guide; Volume 3 - Description of Subroutines; Volume 4 - Verification", NRG report

26094/00.52480/C, Arnhem, October 2000.

- Stem, 2000c M.M. Stempniewicz, "Analysis of PANDA Passive Containment Cooling Steady-State Tests with the SPECTRA Code", *Nuclear Technology*, Vol. **131**, pp. 82-101, July 2000.
- Stem, 2000d M.M. Stempniewicz, "Emergency Shutdown Transient in a Chemical Plant - Analysis with SPECTRA and TRAC Codes", *Chem. Eng.*, to be published.